International Journal of Science and Research (IJSR)
ISSN (Online): 2319-7064
Impact Factor (2012): 3.358

Effect of Preparation Conditions on Anodic Aluminum Oxide (AAO) Shape's and Size

Raad S. Sabry[1], Rahma Alobaid[2]

[1]Almustansiriyah University, College of Science, Physics Department, Baghdad, Iraq

Abstract: ***Anodic aluminum oxide (AAO) template with hexagonal shaped nano-pores with high aspect ratio was fabricated by two-step anodization processes from high purity aluminum foil in oxalic acid solution. AAO template was prepared at different conditions such as voltage and temperature . The electrolyte temperature was kept at 7, 10 and 15 °C, and applied anodizing voltage was 30 and 40 V. It was find that the best ordering occurs at 40 V & at 10 °C ,all the pores were uniform with hexagonal ordered structure. By applying various anodization conditions, AAO templates with pore diameter (30–50nm) and interpore distance varying from 90nm to 110nm were fabricated.***

Keywords: AAO, anodization , nanopores , barrier oxide layer , anodic alumina

1. Introduction

Nanoporous materials have gained much importance in the last 20 years due to their potencial industrial and technological applications for nanometric device fabrication. [1] Anodization of aluminum has been used since the 1920's [2], where it was first used on seaplanes [3]. Anodization increases the resistance of aluminum against corrosion and increases its hardness. This is still an important use of anodization today. In the 1950's another use for the anodization of aluminum became clear when it was discovered that the aluminum oxide formed hexagonal nanopores under certain conditions [4]. In recent years, this possibility to create ordered nanopores has been researched extensively because of its applications in nanotechnology [5].The ordered nanopores offer the possibility to use anodic aluminum oxide as a template for the creation of nanostructured materials

The key features of AAO include simple, inexpensive self-ordering fabrication, large surface area, well-defined and controllable porous structures at the nanometric scale, biocompatibility, easy functionalization of inner pore surfaces, and stable optical, thermal and chemical properties. The combination of these characteristics makes nanoporous AAO a highly attractive material for the development of a broad range of sensing devices for many applications.

Another advantage of using AAO for developing PL-sensing devices is that, unlike other materials (e.g., porous silicon), AAO has a stable PL spectrum and it is not necessary to passivate AAO to prevent changes over the PL spectrum over the course of time .The unique fingerprint of PL in AAO is clearly useful for developing optical sensors, in which a high degree of resolution, sensibility and biocompatibility are required.[6] Synthesis within nanoporous membranes is particularly simple and flexible [7]. In fact, this technique allows producing one-dimensional nanostructures with different aspect ratios and different shapes [8]. In this context, anodic alumina oxide (AAO) is considered an almost ideal "template" for the synthesis of nanostructured materials, to be used in various applications such as optoelectronics, magnetic sensors and electronic circuits [9].In addition, the interest in anodic alumina membranes is also due to the simplicity of their fabrication process. In fact, they can be obtained by anodizing aluminum in appropriate acidic baths, and this leads to the formation of nanoporous honeycomb structures, whose morphological parameters (membrane thickness, pore diameter and density) can be easily controlled by adjusting the anodization parameters (anodization voltage and time, bath temperature and composition)[10].For these reasons, a variety of nanostructures (metals, alloys, semiconductors, oxides and polymers) with different morphologies (tubules, fibers or wires, rods) have been fabricated using AAO as template.[11]

The theory proposed by Jessensky et al.[12] and Nielsch et al,[13] use mechanical stress and the volume expansion associated with the AAO template formation as reasons for self-assembly and ordering. They argue that because the anodization process involves growth of Al_2O_3 on Al, there is volume expansion associated with the process. Further, since on a planar substrate all pores grow at the same time, the Al_2O_3 has nowhere to expand but to rise vertically. This creates mechanical stress in between the cell walls. The equilibration of the stress then leads to the self-ordering behavior of the AAO. Nielsch et al. have further shown that the greatest ordering of the pores occur when moderate increases in volume change occur (~1.2 of the original volume). This volume change corresponds to a porosity of 10%. The porosity rule is found to be true across different electrolytes as well.

The geometry of anodic porous alumina may be schematically represented as a honeycomb structure with a high aspect ratio (depth divided by width) of fine channels characterized by a close-packed array of columnar hexagonal cells, each containing a central pore, as shown in Fig (1) [14].

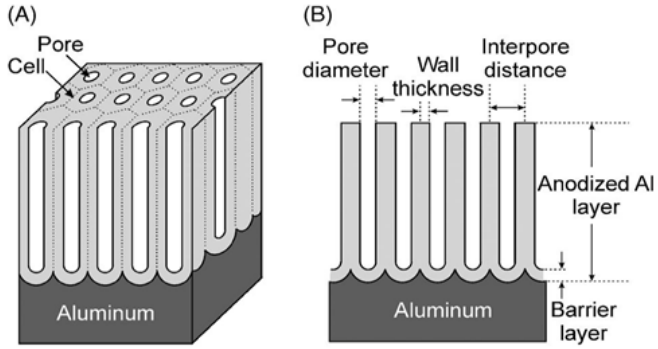

Figure 1: Schematic of an AAO structure.

(A) shows the 3D structure of the pores, the cell structure and the underlying Al.
(B) shows the cross section and the various parameters that define the template.[15]

In all of these studies, it was observed that the growth rate of the pore is highly correlated with the temperature and the anodic voltage. The aim of this paper is to study the effect of temperatures and the anodic voltages for the fabrication of highly ordered pore arrays on aluminum foil , starting from the history of anodization, then the mechanisms of the porous anodic alumina growth and finally our results are shown and compared with the best results available in the literature. Overall this paper indicates on the advantage of the porous anodic alumina system for the growth of nanostructure.

2. Experimental

A pure aluminum foil (purity ~ 99·999%) of thickness 0.5 mm (provided form Alfa Aser) has deep scratches on it, there was first mechanically polished by very smooth sand papers with grit of 1200 and 2000 to obtain a smooth surface .The polished Al was degreased in acetone , methanol and deionized water by ultrasonication for 30 min to remove any adhering surface impurities , followed by a cleaning step consisting of 5 % NaOH solution for 30 seconds at room temperature to remove the native oxide. Then , the foil was rinsed with deionized water for five minutes. It is also important that the Al foil should be annealed for at least 5 h at 550 $^{\circ}$C ,which helps in the removal of crystal defects and promotes grain growth as shown in fig(2.a).By mechanical polishing, deep scratches of aluminum foil are removed, but there are still some defects and protuberance of the surface. The surface roughness of the annealed Al surface is reduced to nearly 3 nm [1] by electro polishing the aluminum foil in a standard acidic electrolyte containing of $HClO_4$ (60%) and ethanol (99.5%) (V/V 1:4) at 20 V for 4 min at 10 $^{\circ}$C to obtain a surface like mirror as shown in fig(2.b). Finally, the foil was rinsed with deionized water several times in order to remove completely the polishing solution and the foil becomes ready for the anodization process. The Al foil was used as anode while Pt wire was used as a cathode. The distance between two electrodes was kept at 4cm as shown in fig(3). Two-step anodization was carried out in 0.3M $C_2H_2O_4.2H_2O$ solution[14,15]. To obtain the optimum condition for ordered hexagonal pore structure, the electrolyte temperature, anodization voltage and duration of the anodization were varied. Temperature of the bath was kept at 7, 10 and 15 $^{\circ}$C, and applied anodizing voltage was 30 & 40V.The first anodization was carried out for 5h with constant temperature and anodizing voltage as shown in fig(2.c). After the 1st anodization, AAO layer was etched out in 6 wt% phosphoric acid (H_3PO_4) and 1.8 wt% chromic acid (CrO_3) at 60–80 $^{\circ}$C for 30–45 min as shown in fig(2.d).The second anodization was carried out for 2h under same condition as the first as shown in fig(2.e). During the anodization, the electrolyte should be vigorously stirred to effectively remove hydrogen bubbles and local heat on the surface, and to allow a homogenous diffusion of anions into pore channels and helps AAO to be better ordered since the concentration profile along pore axis is influenced by electrolyte agitation. The unreacted aluminum was detaching from the AAO template by dipping the foil in a $CuCl_2$ solution (5 gm $CuCl_2.2H_2O$ + 100 ml H_2O) at 30 $^{\circ}$C for about 1 hour as shown in fig(2.f) .The detached AAO template cleanes carefully with DI water to remove residues of metal ions .The structure of the AAO template was then investigated by field emission scanning electron microscopy(FESEM,HitachiS-4160)

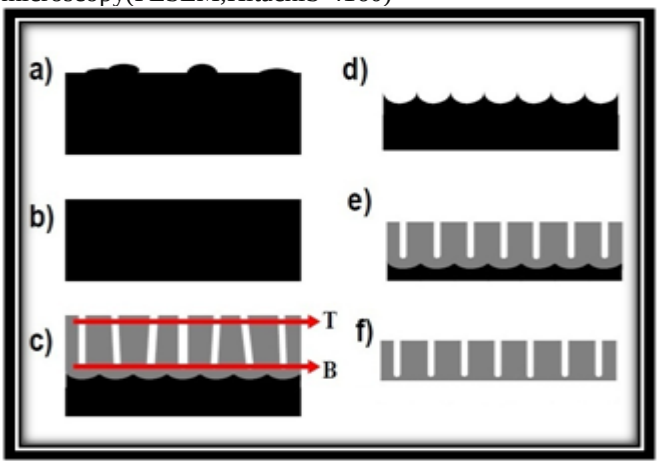

Figure 2: Stages of the formation of self-ordered alumina.[16]

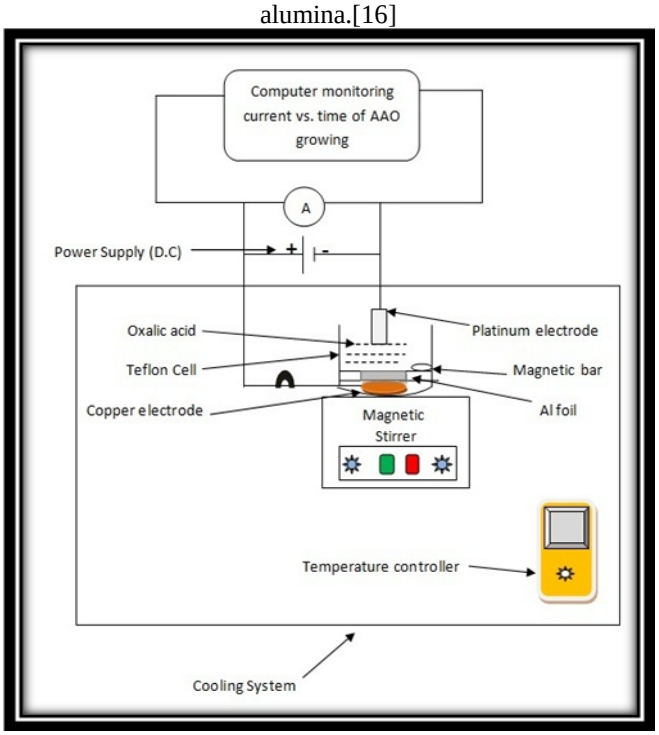

Figure 3: Schematic diagram of the electrochemical cell

3. Results & Discussion

The AAO nano templates can be created by one-step, two-step or three-step anodization process, but as asserted by Masuda et al. [1] the two-step anodization process appears to be the best choice as it results in high control of the nanostructure of the AAO such as its regularity and size. Self-organization has been found with three types of aqueous electrolytes: sulfuric acid (H_2SO_4), oxalic acid ($H_2C_2O_4$) and phosphoric acid (H_3PO_4). It is well known that among sulfuric acid (H_2SO_4), oxalic acid ($H_2C_2O_4$), and phosphoric acid (H_3PO_4), oxalic acid is the best for the growth of aluminum oxide in terms of size and regularity of the pore [17]. In the present work, we have chosen oxalic acid as a fixed parameter for the oxidation process. The pore diameter was dependent on the anodization voltage and temperature. The depth of the AAO template is proportional to the second anodization time. A longer anodization time favored not only increasing the pore depths but also extending the uniformity of the AAO membrane. During the 1st anodization, hexagonal pores formed on the surface of Al foil are non-ordered due to the surface roughness .These non-ordered pores of AAO foil should be removed by wet chemical etching using a mixture of phosphoric and chromic acids[18] .Removal of the porous film from the Al foil leaves behind an ordered concave textured structure on the sample surface. During this second step anodization process, the concave textured pattern on the aluminum foil surface acts as the sites for deep pore growth and is helpful in growing the porous oxide film uniformly [19]. The transient of the potentiostatic current density reflects the formation of barrier-type or porous type porous alumina .At the beginning of the oxide formation, both transients have an identical behavior. However, for the barrier film formation, the current density j_b decays exponentially. Eventually, the barrier film current is dominated by an ionic current j_i. In the case of the formation of porous films, the following current density profiles are typically observed. At the beginning of the anodization, the current density j_p decreases rapidly, the barrier film which consists of non-conductive oxide covers the entire surface of the aluminum surface (regime 1). Then, it passes through minimum value , the electric field is focused locally on fluctuations of the surface (regime 2). It increases to arrive at a maximum value, this leads to field-enhanced or/and temperature-enhanced dissolution in the formed oxide and thus to the growth of pores (regime 3). Subsequently, it slightly decreases again, Since some pores begin to stop growing due to competition among the pores. Finally, j_p maintains an equilibrated state. In this stage, pores grow in a stable manner. However, it is very often observed that during the stable pore growth, the current density continues to decrease slightly. This is due to diffusion limits in the long pore channels (regime 4).

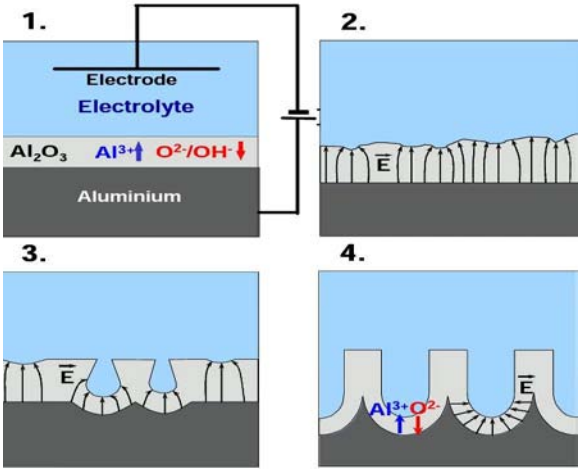

(a)

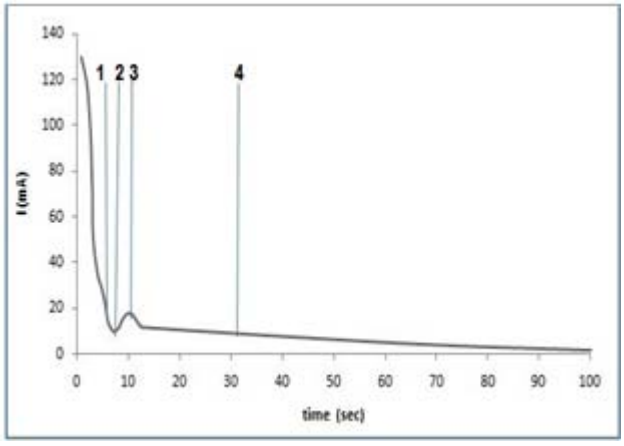

(b)

Figure 4: Current versus time of all four steps of (a) pore growth.[20] (b) schematic diagram of these four steps.(Our study)

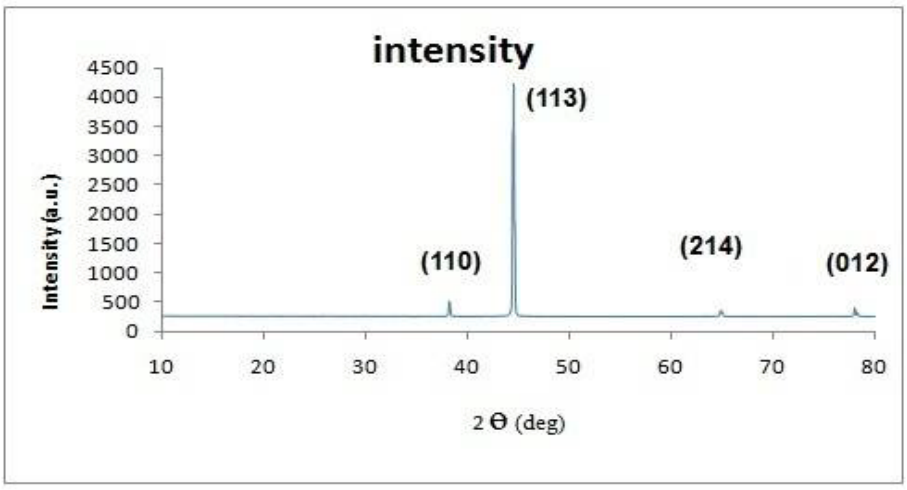

Figure 5: X- Ray diffraction pattern of AAO at 40 V & 10 °C.

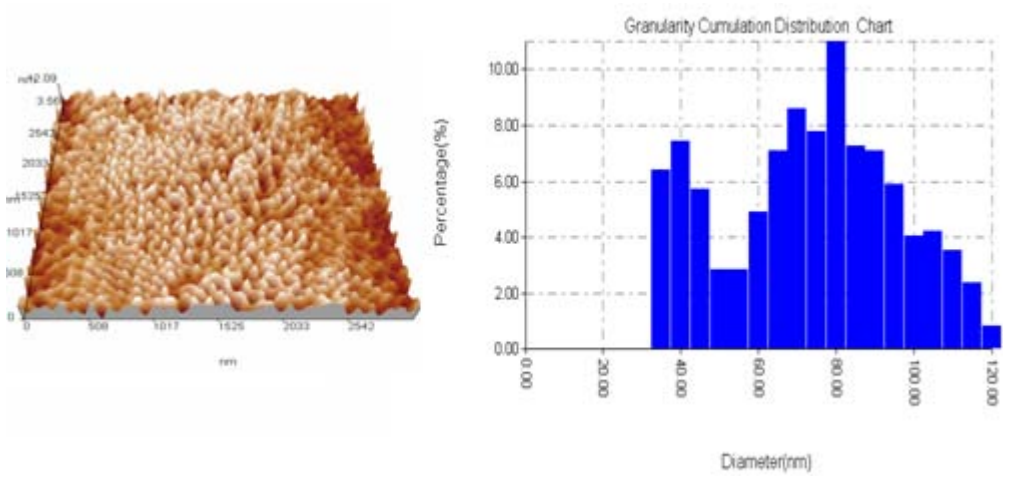

(a)

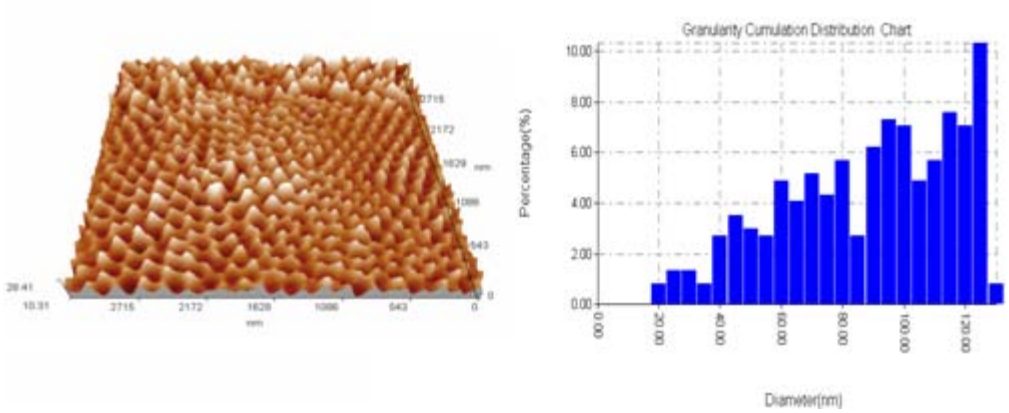

(b)

Figure 6: AFM images for top view of pore arrays.
(a) at 30V & 10 °C .
(b) at 40V & 10 °C .

Table 1:

Condition	R_a (Roughness average)	RMS (Root Mean Square)	Sz (Ten Point Height	D_P (Pore Size)
30V & 10 °C	1.42 nm	1.74 nm	8.53 nm	25 nm
40V &10 °C	2.87 nm	3.57 nm	18.1 nm	37 nm

From Fig (6) & Table (1), We observed that the pores are clearly, homogeneous distribution ,peaks approximately equal, the roughness increase with temperature and voltage increasment and wherever the number of pores increase , the roughness increases also. Almost perfect hexagonally arranged pore domains can be seen. The pores with a narrow size distribution are surrounded by six columnar oxides, which are interconnected to form a network structure. During the period of the observation, the boundary of the domain appeared in the large scale, which perhaps resulted from the formation process of the pores. All the pores were uniform with hexagonal ordered structure.

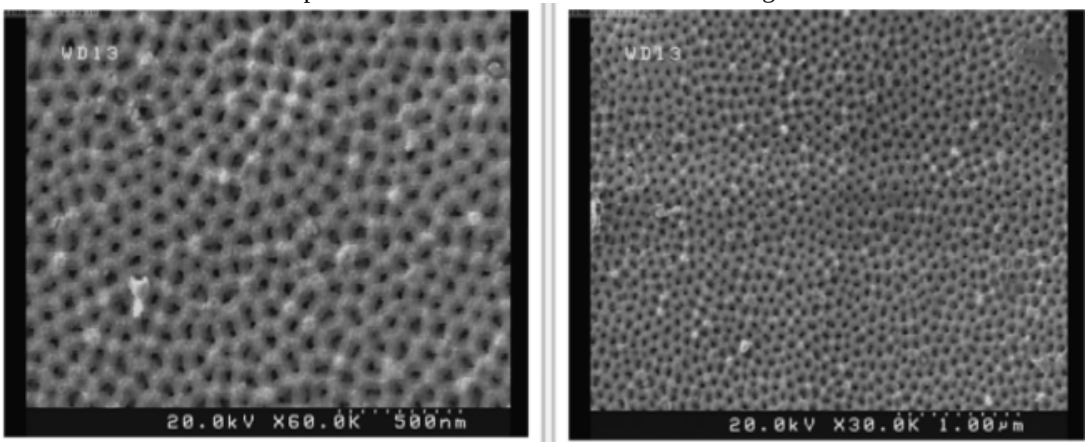

(a)

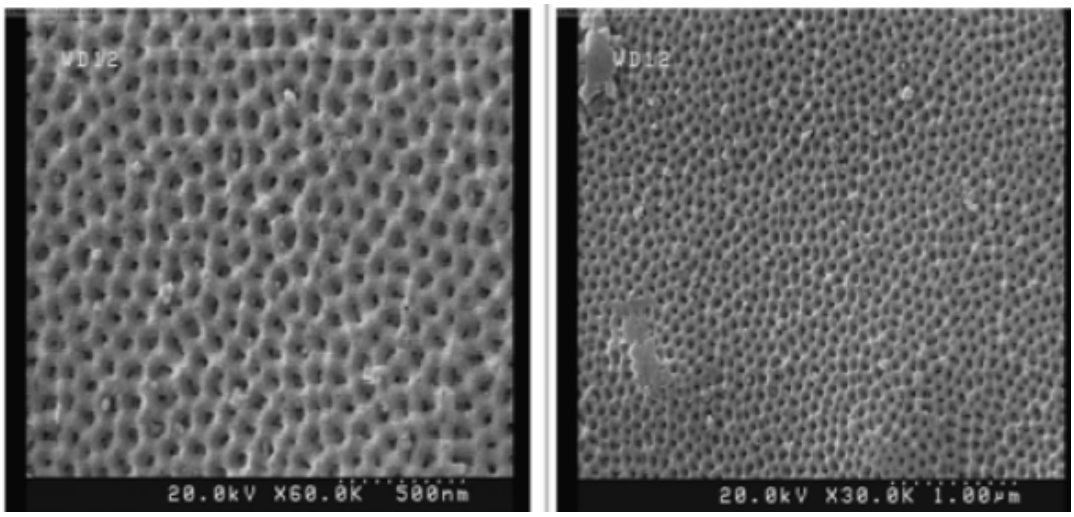

(b)

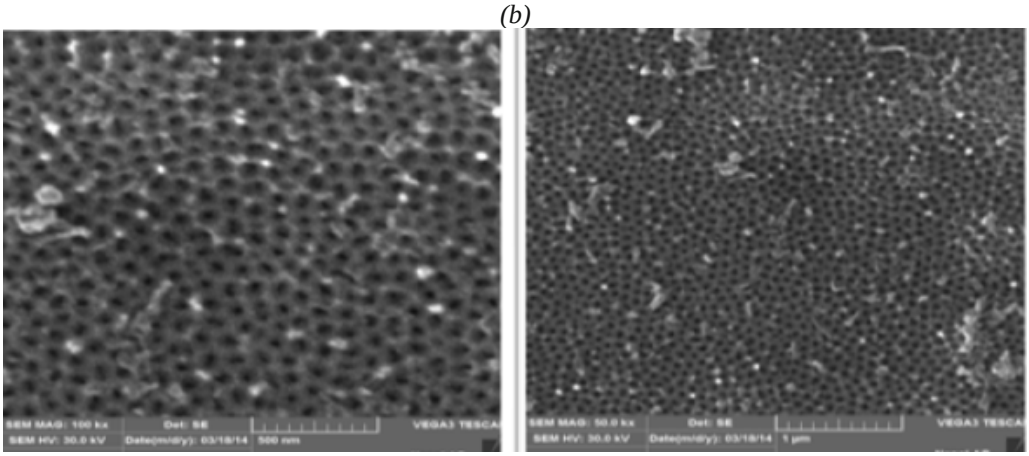

(C)

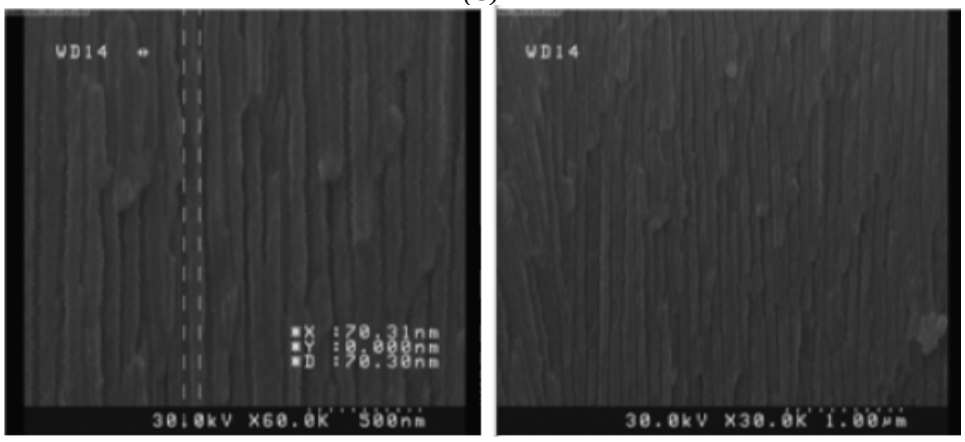

(d)

Figure 7: FESEM images of the top surfaces after second anodization.
(a) at 7 °C & 40V.
(b) at 10 °C & 40V.
(c) at 15 °C & 40V .
(d) cross section of AAO template.

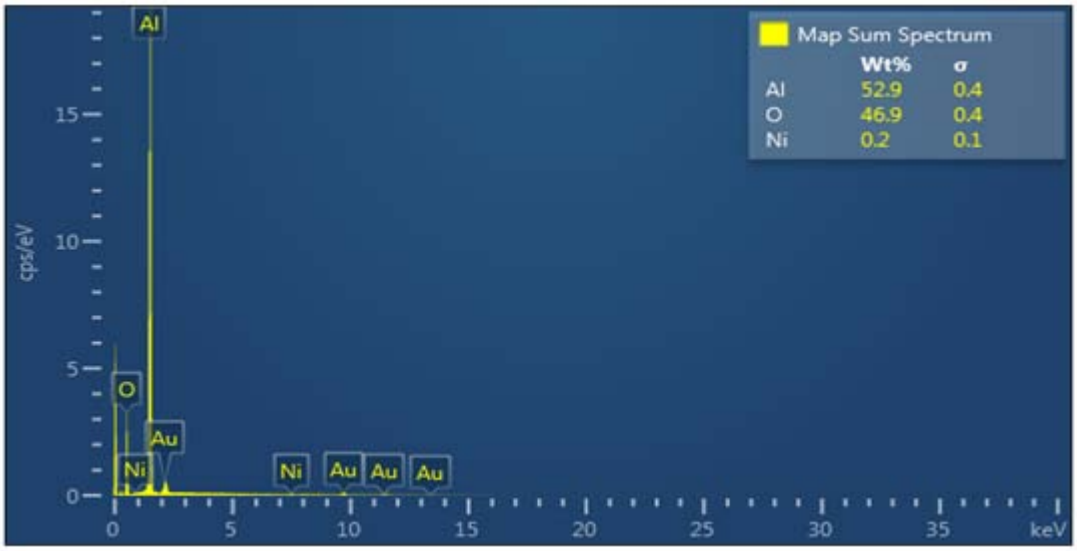

Figure 8: Energy-dispersive X-ray spectroscopy (EDS, EDX, or XEDS).

The Barrier layer thickness (D_{BL}) can be calculated approximately by the following equ.[21]: $\boldsymbol{D_{BL} = \alpha_1 + \alpha_2 .V}$ where α_1= 5.9 nm and α_2= 0.9 nm V^{-1}(values of α_1 and α_2 are valid for oxalic acid templates at voltage 40V). D_{BL} is about 41 nm

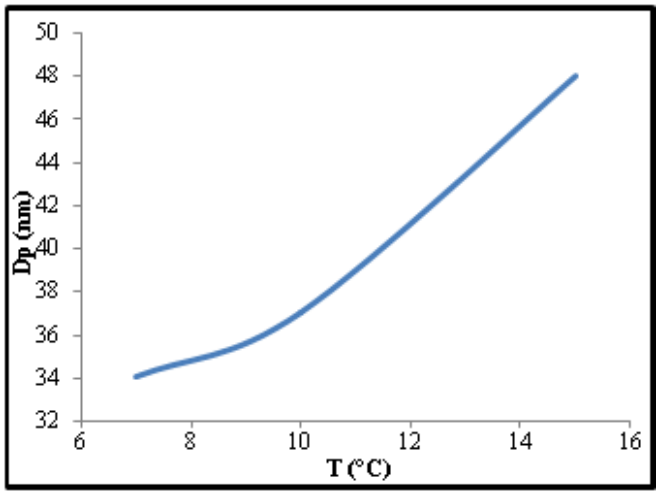

Figure 9: Variation of the pore diameter as a function of temperature

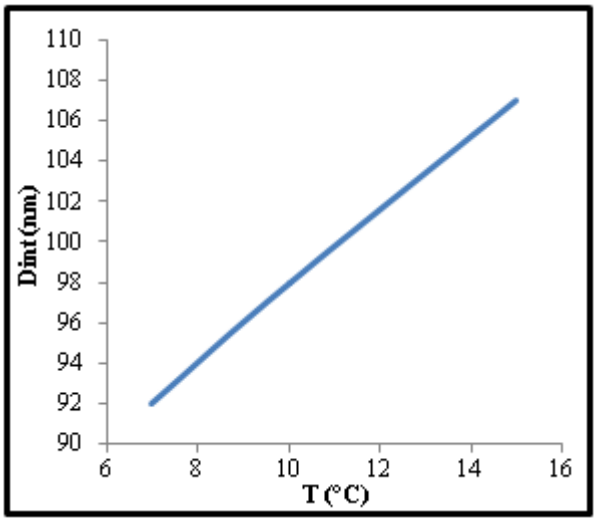

Figure 10: Variation of the interpore distance as a function of temperature.

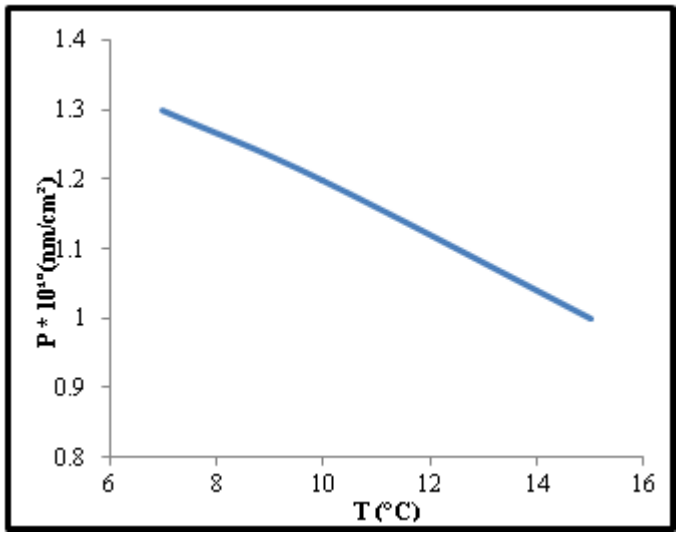

Figure 11: Variation of the porosity (pore density) as a function of temperature.

Table 2: The diameter of pore, interpore distance and the porosity of AAO template growing at different temperatures.

Electrolyte Temperature T (°C)	Pore diameter D_p (nm)	Interpore distance D_{int} (nm)	Porosity P $*10^{10}$ (nm/cm^2)
7	34	92	1.3
10	37	98	1.2
15	48	107	1

The applied potential V, is one of the most important factors to adjust self-assembly of porous alumina. The anodization voltage plays a crucial role influencing the pore diameter. In addition, the oxide layer at the bottom of pores could be controlled by changing the anodization voltages. During anodization at a constant DC voltage, the thickness of the barrier oxide layer remains constant, because the rate of alumina dissolution on the electrolyte side is equal to the rate of alumina production on the metal side. At lower voltage, the barrier oxide layer is quite thick; that led to small pore size and higher voltage led to large pore size because the barrier oxide layer is thin. However, for the other experiments the value of the anodization voltage has

been set at 40V, because it results in the largest pore size and the highest pore density without losing the regularity of the structure and to obtain the best quality of AAO template.[22] In order to know the effect of temperature on the pore size the temperature is kept constant during anodization of each AAO. It was noticed that the anodizing current increased with the temperature. When we increase the temperature ,the pore diameter of the pores increase by using the two-step anodization process. During the anodization, temperature should be kept lower than room temperature to prevent the formed oxide structure from being dissolved in acidic electrolytes. A second reason to keep the temperature as low as possible is to avoid a local heating at the bottom of the pores during the course of anodization (specially, in the case of anodization at a high potential). The local heat causes an inhomogeneous electric field distribution at the bottom, leading to local electrical breakdown of the oxide . In fact, cracks and bursts of the oxide film are generated if porous alumina is formed without temperature controlling. If the temperature is too low (just below zero degree) and diluted electrolytes are used, the electrolyte may freeze. In addition, the speed of the growth of porous alumina is affected by the temperature. The lower the temperature, the lower is the growth rate.

However, in all the cases the anodization temperature is purposely kept low, preferably below the room temperature because, high bath temperature enhances the dissolution of porous oxide film in the electrolyte. The heat generation is harmful to nanostructures because it accumulates randomly all over the AAO structure especially the discontinuous geometry to enhance the dissolution effect. [23] It was found that a long anodization time can improve the regularity of the cell arrangement. Defect free regions appear in large domains whereas defects are found at the boundaries of these domains. That means the size of the defect free region increases with the anodization time. Even at the deficiency site of the concave pores configuration can be recovered after a long anodization period. This is because the pores at deficient sites tend to develop and recover the closed packing arrangement of the cylindrical cells, which is the most probable arrangement in the cell configuration and leads to the thicker of AAO template.[24,25]

4. Conclusion

AAO templates were produced under various conditions of electrolyte temperatures and anodizing voltages. The vertical growth rate of pores was found to vary exponentially with anodizing voltage in comparison with linear variation with respect to the electrolyte temperature. It is found that through variation voltage and temperature , we conclude that the best result was achieved at 40 V and 10 $^{\circ}$C to obtain highly ordered hexagonal nanopores of AAO template. The AAO templates with different pore diameters and thicknesses were successfully fabricated for the growth of nano dimensional materials using both wet ,dry deposition techniques and PL sensing devices.

References

[1] Masuda H., Fukuda K., *Science*, (1995) 1466.
[2] G. D. Bengoughand and J. M. Stuart, “Br. pat., 223994,” 1923.
[3] G.E.J. Poinern, N. Ali, and D. Fawcett, “Progress in nano- engineered anodic aluminum oxide membrane development,” *Materials*, vol. 4, no. 3, pp. 487–526, 2011.
[4] F. Keller, M. S. Hunter, and D. L. Robinson, “Structural features of oxide coatings on aluminum,” *Journal of The Electrochemical Society*, vol. 100, no. 9, pp. 411–419, 1953.
[5] G. D. Sulka, *Highly Ordered Anodic Porous Alumina Formation by Self-Organized Anodizing*, pp. 1–116. Wiley-VCH Verlag GmbH & Co. KGaA, 2008.
[6] A. Santos, G. Macı´as, J. Ferre´-Borrull, J. Pallare`s, L.F. Marsal, ACS Appl. Mater. Interfaces 4 (2012) 3584.
[7] Martin C. R., 1996, Membrane-Based Synthesis of Nanomaterials, Chem. Mater., 8, 1739-1746.
[8] Inguanta R., Ferrara G., Piazza S. and Sunseri C., 2009a, Nanostructures fabrication by template deposition into anodic alumina membranes, Chem. Eng. Trans. 17, 957- 962.
[9] ShingubaraS.,2003, Fabrication of nanomaterials using porous alumina template, J. Nanopart. Res. 5, 17-30.
[10] Inguanta R., Butera M., Sunseri C. and Piazza S., 2007a, Fabrication of metal nanostructures using anodic alumina membranes grown in phosphoric acid solution :Tailoring template morphology, Appl. Surf. Sci. 253, 5447-5456.
[11] Zhang G. and Chen J., 2005, Synthesis and Application of La0.59Ca0.41CoO3 Nanotubes, J Electrochem. Soc. 152, A2069-A2073.
[12] O. Jessensky, F. Muller, U. Gosele, *Applied Physics Letters* **1998**, *72*, 1173.
[13] K. Nielsch, Choi, J., Schwirn, K., Wehrspohn, R.B., Gosele, U., *Nano Lett.* **2002**, *2*, 677.
[14] A.Eftekhari,Ed. *Nanostructured Materials in Electrochemistry*, Wiley-VCH Verlag GmbH & Co., **2008**.
[15] Hwang S K, Jeong S H, Hwang H Y, Lee O J and Lee K H 2002 *Korean J. Chem. Eng.* **19** 467.
[16] P. Larson, "Fabrication and characterization of ordered arrays of nanostructures," *.Ph.D. dissertation, University of Oklahoma, United States, Oklahoma.*, 2005.
[17] J. Siejka and C. Ortega, J. Electrochem. Soc. **124**, 833, (1997).
[18] Ma D, Li S and Liang C 2009 *Corros. Sci.* **51** 713.
[19] (Masuda et al 1997).
[20] Choi J., *Dissertation*, (2004).
[21] J. P. O' Sullivan, G. C. Wood, *Proc R Soc Lon Ser-A* **1970**, *317*, 511.
[22] J.P. O’Sullivan and G.C. Wood, Proc. R. Soc. London, Ser. A. **317**, 511 (1970).
[23] K. Yokoyama, H. Konno, H. Takahashi, and M. Nagayama, Plating and Surface Finishing 69 (1982) 62-65.
[24] W.Q. Han, S.S. Fan, Q.Q. Li and Y.D. Hu, Science **277**, 1287 (1997).
[25] D. Routkevitch, A.A. Tager, J. Haruyama, D. Almawlawi, M. Moskovits and J.M. Xu, IEEE. Trans. Electron Devices. **43**, 1646 (1996).